NENE 2015 September 14-17 PORTOROŽ SLOVENIA
24th International Conference Nuclear Energy for New Europe

Assessment of NEPTUNE_CFD Code Capabilities to Simulate Two-Phase Flow in the OECD/NRC PSBT Subchannel Experiments

Sergii Lutsanych, Fabio Moretti, Francesco D'Auria
University of Pisa, San Piero a Grado Nuclear Research Group (GRNSPG)
Via Livornese 1291
56122, San Piero a Grado, Pisa, Italy
s.lutsanych@ing.unipi.it, f.moretti@ing.unipi.it, f.dauria@ing.unipi.it

ABSTRACT

This paper deals with the validation of the multifield computational fluid dynamics code NEPTUNE_CFD v2.0.1 against experimental data available from the OECD/NRC NUPEC PWR subchannel and bundle tests (PSBT) international benchmark. The present work is performed in the framework of the NURESAFE European collaborative project and focuses on the steady-state single subchannel void fraction tests.

From overall 126 PSBT experiments covering wide range of test conditions and 4 different geometrical configurations of PWR subchannel, 42 tests have been selected and simulated using NEPTUNE_CFD. Following the NEA/CSNI (Nuclear Energy Agency / Committee on the Safety of Nuclear Installations) best practice guidelines about computational grid design and grid quality, mesh sensitivity analysis has been performed using axial and radial grid refinement. Both axial and radial mesh sensitivity studies do not exhibit any significant change in the predicted results, which thus result to be grid-converged. Besides, a series of sensitivity calculations have been performed in order to investigate the influence of uncertainties of the experimental boundary conditions on the code predictions.

The influence of code physical and closure models on the void fraction prediction has been studied and discussed in detail. Generally, the calculated cross-sectional averaged void fraction at the measurement plane differs from the measured one by maximum of +/- 8%. This discrepancy is comparable to the 2σ experimental uncertainty range on void fraction measurement. The performed investigations have shown the ability of NEPTUNE_CFD to predict reasonably the void fraction in PSBT subchannel using appropriate modelling.

1 INTRODUCTION

The OECD/NRC NUPEC PWR subchannel and bundle tests (PSBT) International Benchmark [1], was organized by OECD/NEA and US NRC to assess the capabilities of system thermal-hydraulic codes, subchannel codes, and computational fluid dynamic codes to predict detailed void distributions and departure from nucleate boiling in subchannels on the basis of experimental data measured at a full-scale prototypical PWR rod bundle in NUPEC test facility.

One of the outcomes of this benchmark was the disclosure of a set of experimental data that can be used for the validation of numerical models of void-fraction distribution over wide range of operating conditions, and for the development of novel approaches. A part of such data was already used for similar purposes during the NURISP project; in particular, a few tests were used for the validation of NEPTUNE_CFD v1.0.7 (e.g. [2], [3] etc.).

It is thus deemed useful to challenge the new version of the code on a larger number of tests from the same database spanning over operating ranges as wide as possible, so as to contribute to the systematic and thorough assessment of the code and of the specific models involved.

The activity described in the present paper focuses on the validation of the NEPTUNE_CFD v2.0.1 code against experimental data available from PSBT steady-state subchannel tests on void fraction (VF) distribution.

2 CONTRIBUTION TO THE VALIDATION OF NEPTUNE_CFD CODE

2.1 The NEPTUNE_CFD Code General Overview

NEPTUNE_CFD [4] is a 3-D multifield CFD code developed within the NEPTUNE multiscale thermal-hydraulic platform, financially supported by CEA (Commissariat à l'énergie atomique et aux énergies alternatives), EDF (Electricité de France), IRSN (Institut de Radioprotection et de Sûreté Nucléaire) and AREVA-NP. This code has been designed for nuclear reactor applications and mainly devoted to bubbly and separate-phase flows.

The NEPTUNE_CFD solver is based on a pressure correction approach simulating multi-component multiphase flows by solving a set of three balance equations for each field (fluid or gas phase). The spatial discretization adopts fully-unstructured finite-volume approach with a collocated arrangement of all variables. Details about the NEPTUNE_CFD models and closure laws can be found in the code's theory and user guide ([5], [6]).

2.2 Scope and Description of OECD/NRC PSBT Benchmark

The present work considers the PSBT steady-state experimental tests [1] measuring the void fraction on four subchannel-type test assemblies (S1, S2, S3, and S4) which simulate the subchannel types (central, central with thimble, side, and corner) in a PWR assembly (Figure 1). The effective heated length is 1555 mm, and the void measurement section is located at 1400 mm elevation. The external diameter of the rod is 9.5 mm; the rod pitch and the rod gap measure, respectively, 12.6 mm and 3.1 mm. The heating power is uniformly distributed.

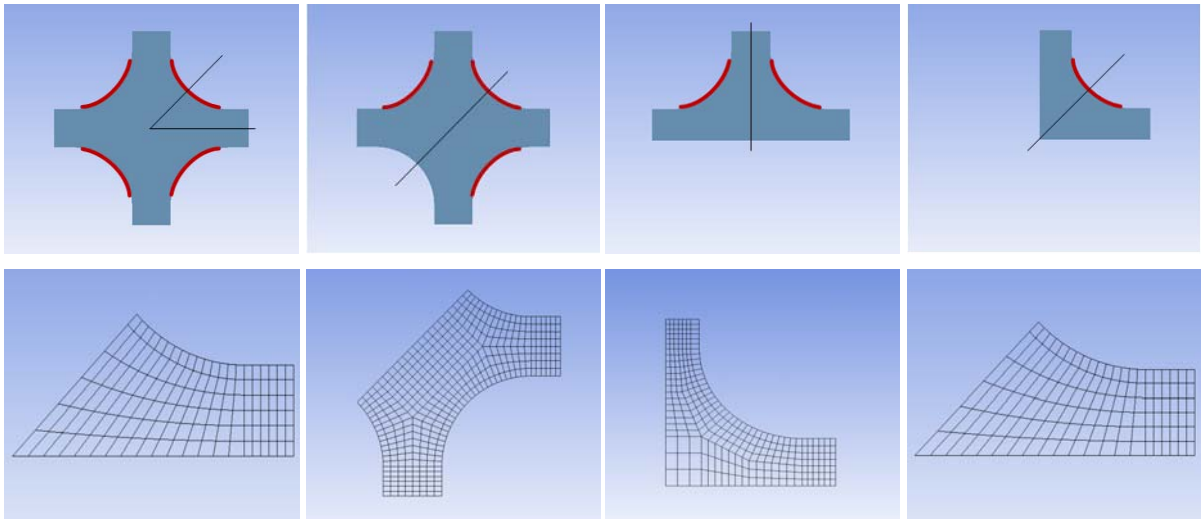

(a) S1 (b) S2 (c) S3 (d) S4

Figure 1: Cross-section view of grid for subchannel type S1 – S4

2.3 Space Discretization of PSBT Subchannel

Following the NEA/CSNI best practice guidelines for the use of CFD in Nuclear Reactor Safety [7], four fully structured hex meshes have been developed to represent geometrical configuration of the subchannel S1, S2, S3 and S4 respectively (Figure 1(a)-(d)). Owing to the simple geometry and to the axial symmetry of the problem, the computational domain is reduced depending on the geometry of considered subchannel. The cells in the near wall region are thinner in order to describe the velocity and temperature gradients more accurately. Geometrical aspects of the spatial discretization are summarized in Table 1.

Table 1: Characteristics of the grids used in the simulations

Item	Subchannel Type			
	Typical (S1)	Thimble (S2)	Side (S3)	Corner (S4)
Total number of cells	26880	133760	92480	40320
Number of cells in axial direction	320	320	320	320
Cell size in axial direction (mm)	5	5	5	5
First cell near the wall (mm)	0.4	0.4	0.4	0.4
Number of cells in X-direction	12	20	23	21

2.4 Computational Model Set-up

The turbulence of the liquid phase is modelled using a first-order, standard k-ε RANS (Reynolds-Averaged Navier-Stokes) model. Large spherical inclusions model is activated for the vapour phase. The interfacial momentum transfer is considered as the sum of the following five contributions: the drag force (by Ishii and Zuber correlation [8]), the added mass force (by Zuber [9] expression), the lift force (by Tomiyama et al. [10]), the turbulent dispersion force (by using Generalized Turbulent Dispersion closure) and the wall lubrication force (by Tomiyama formulation). The interfacial area concentration is modelled by using the Yao-Morel formulation [11] with maximum bubble diameter 0.5mm.

The wall-to-fluid heat transfer at nucleate boiling is modelled by the Extended Kurul & Podowski model [12], which consists in splitting the heat flux into three terms: one heating the liquid phase in contact with the wall, one responsible for the bubble generation, and the last one arising from the arrival of liquid water at the wall, caused by bubble departure. A fourth flux is introduced to take into account the convective heat transfer transmitted to the vapour (at higher VF). To ensure a grid independent solution, the liquid temperature in the wall boiling equations is calculated from the logarithmic profile in a given nondimensional distance from the wall at y+ = 250 (this solution is proposed by Egorov and Menter [13]).

2.5 Boundary Conditions

In the present validation study, 42 PSBT tests out of 126 have been calculated: 12 tests for assembly type S1 and 10 tests for each assembly type S2-S4. The boundary conditions of the selected PSBT steady-state experimental tests vary in the following ranges: Pressure from 73 bar to 166 bar, Inlet Mass Flux from 1369 kg/m^2/s to 4133 kg/m^2/s, Wall Heat Flux from 1077 KW/m^2 to 1939 KW/m^2, and Inlet Subcooling from 5.8K to 70.8K. Figure 2 shows an example of application of the boundary conditions to subchannel type S1.

In order to reach the steady-state, a null-transient is performed for each simulation case. It is based on heat-up conditioning phase during which power of the fuel rod simulators is increasing linearly from 0 to the nominal value and stabilizing phase (at constant power). This approach together with adopted uniform time step scheme allows to reduce the numerical instabilities and to have smoother convergence of the iterative numerical algorithm.

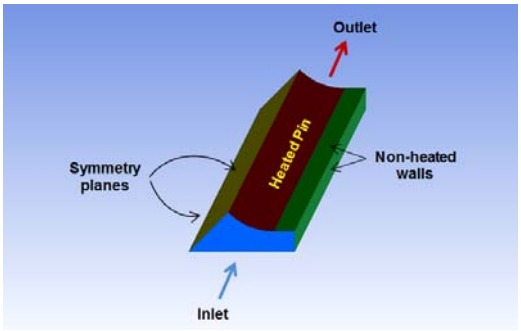

Figure 2: Boundary conditions (subchannel type S1)

2.6 Base Calculation of the PSBT Test 1.2211

The PSBT run 1.2211, whose operating conditions [1] are the closest to PWR normal conditions, has been selected and used to develop a reference simulation model for PSBT tests with a subchannel of type S1. The results of this test are shown in Figure 3 - Figure 4.

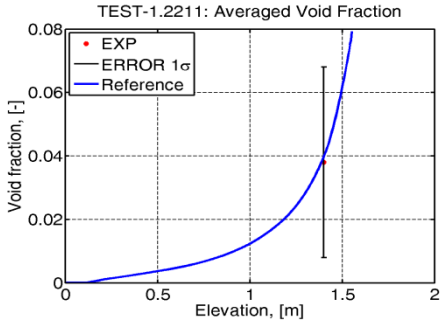

Figure 3: Axial evolution of cross-section averaged void fraction

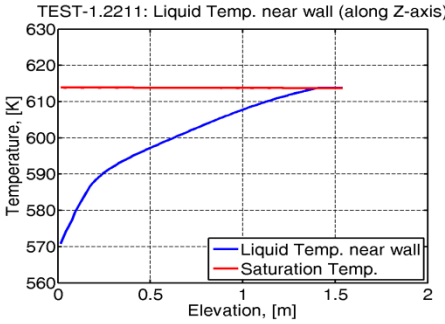

Figure 4: Axial evolution of liquid temperature at the near wall region

3 SENSITIVITY ANALYSES

3.1 Effect of the Computational Grid

Following the NEA/CSNI best practice guidelines about the computational grid design and grid quality [7], mesh sensitivity analysis based on PSBT test 1.2211 has been performed using axial and radial grid refinement (Table 2). The results of calculations obtained with the reference set of physical and closure models are shown in Figure 5 - Figure 7.

Table 2: Characteristics of the grids used in the axial and radial sensitivity studies

Item	Axial Sensitivity				Radial Sensitivity		
	0.2mm-200AX	0.2mm-320AX	0.2mm-400AX	0.2mm-800AX	0.2mm-200AX	0.3mm-200AX	0.4mm-200AX
Total number of cells	16800	26880	33600	67200	42000	21000	21000
Number of cells in the axial direction	200	320	400	800	200	200	200
Cell size in the axial direction (mm)	8	5	4	2	8	8	8
First cell near the wall (mm)	0.2	0.2	0.2	0.2	0.2	0.3	0.4
Number of cells in X-direction	12	12	12	12	21	21	21

Axial mesh sensitivity calculations do not exhibit any significant change (Figure 5(a) - Figure 7(a)). However, in order to avoid high grid aspect ratios and to have reasonable computational time, the grid with 320 axial meshes was selected as reference. Radial mesh sensitivity shows that void production in the near heated wall region is higher for the smaller computational cells (Figure 6(b)). It may be explained by larger diameter of the bubbles that

are generated in that region by refined grid (Figure 7(b)). Similar results were obtained by Baudry et al. [11]. In order to minimize a computational cost of the calculations while preserving the numerical stability of the code, the coarse grid with 0.4mm wall-adjacent cell was selected as the reference one. The nondimensional distance from the wall y+ is varied in the range of approximately 120 (PSBT test 1.4326) up to ~300 (PSBT test 1.2211), which is valid for the application of the selected *k-ε* turbulence model [6].

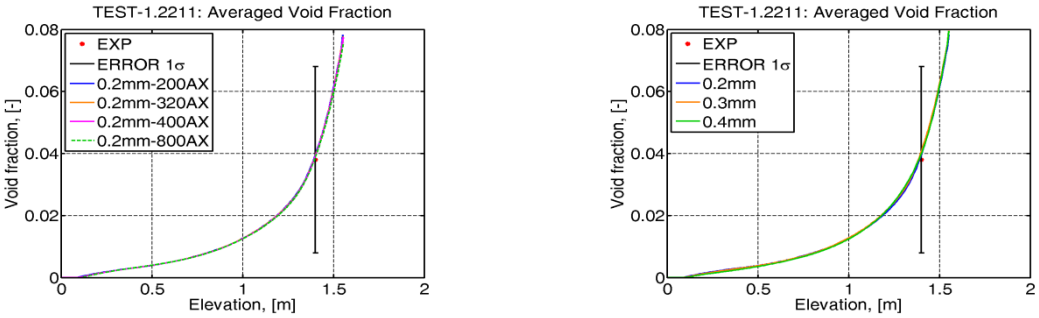

a) Axial Mesh Sensitivity b) Radial Mesh Sensitivity

Figure 5: Axial evolution of cross-section averaged void fraction (PSBT test 1.2211)

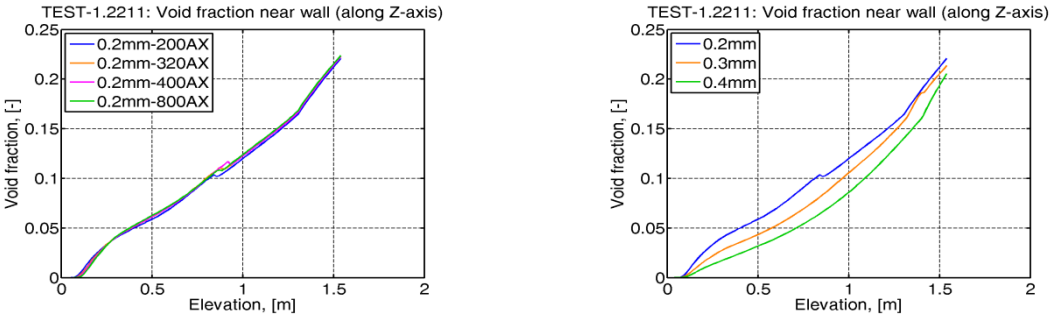

a) Axial Mesh Sensitivity b) Radial Mesh Sensitivity

Figure 6: Axial evolution of void fraction at the near wall region (PSBT test 1.2211)

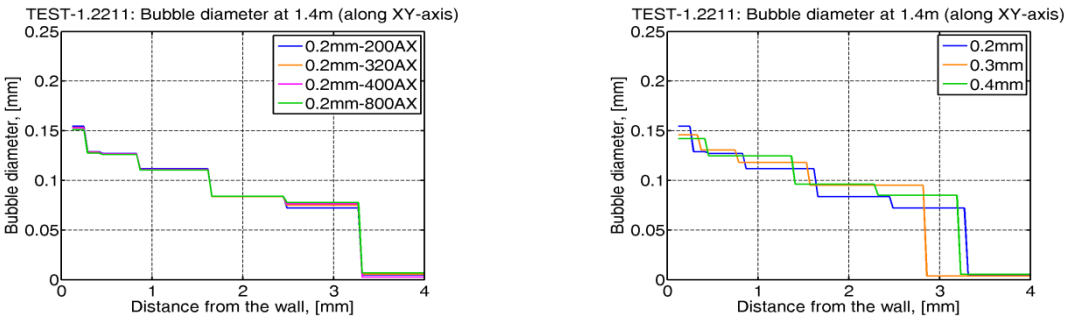

a) Axial Mesh Sensitivity b) Radial Mesh Sensitivity

Figure 7: Bubble diameter size in the near wall region at 1.4m (PSBT test 1.2211)

3.2 Effect of the Boundary Condition Variations

Series of sensitivity calculations of PSBT test 1.2211 have been performed in order to assess the influence of experimental uncertainties of the boundary conditions (BC) on NEPTUNE_CFD predictions. The procedure is based on single-parameter variation of the BC in range of nominal value plus or minus the value of corresponding uncertainty, meanwhile not changing other parameters. Two additional calculations have been run in order to find the widest possible span of variation of the averaged void fraction. It is achieved by using two opposite set of parameters that give the highest or the lowest values of void fraction. The results of sensitivity studies are shown in Table 3.

Table 3: Effect of the BC experimental uncertainties on the predicted void fraction

PSBT test 1.2211	
Exp. values (α_{exp})	0.038
Calc. values (α_{ref})	0.040
Inlet Temp. ± 1K	$\alpha_{ref} \pm 0.005$
Inlet Mass Flux ± 1.5%	$\alpha_{ref} \pm 0.004$
Pressure ± 1%	$\alpha_{ref} \pm 0.005$
Wall heat flux ± 1%	$\alpha_{ref} \pm 0.002$
Inlet T-1K, Inlet MF+1.5%, P+1%, WHF-1%	$\alpha_{ref} - 0.015$
Inlet T+1K, Inlet MF-1.5%, P-1%, WHF+1%	$\alpha_{ref} + 0.025$

The 0.04-wide range in case of multi-parameter variation represents approximately 50% scatter range of the experimental value. Similar results were drawn by Peréz et al. [3]. Generally, it can be concluded that experimental uncertainties on the BC parameters may have considerable effect on the simulation results (especially for highly subcooled tests).

3.3 Effect of the Bubble Size Description

Influence of the bubble size description on the calculated results has been studied by performing simulations of PSBT test 1.2211 using interfacial area models of Yao-Morel and Ruyer-Seiler. Besides, four different simulations with constant and uniform predetermined bubble diameters (0.05mm, 0.1mm, 0.2mm and 0.3mm) were carried out. The results of calculations are presented in Figure 8 - Figure 11.

The Yao-Morel model [11] is based on so-called “single-size” approach for bubbly flows. It supposes that bubbles have locally (i.e. in the same computational cell) the same size, represented by the Sauter mean diameter, which is directly connected to the local void fraction and to the interfacial area. The Ruyer-Seiler model [14] may be considered as more refined than the Yao-Morel model since it follows the “moment-density” approach. It consists in assuming a certain form for the bubble diameter distribution function (other than a delta Dirac distribution), and then solving equations on the moments defining this distribution. In this model, coalescence and break-up phenomena are taken into account.

As illustrated in Figure 8, the highest averaged void fraction on the whole heated length of the subchannel is obtained in the simulation with a constant bubble size of 0.3mm, while the lowest one with the 0.05mm bubble size. The two bubble-size models exhibit nearly-similar behaviour and show better general agreement with the experiment at the location of measuring section (1.4m). The bubble diameter calculated at this elevation by Yao-Morel and Ruyer-Seiler models is lower than that in case of calculation with fixed bubble diameter of 0.2mm and 0.3mm (Figure 11). The bubble size in this region obtained by Ruyer-Seiler model (~0.2mm) is higher than the one predicted by Yao-Morel model (~0.15mm).

Void fraction within subcooled region near the heated wall is decreasing when reducing size of the bubbles (Figure 9). Smaller bubbles yield bigger interfacial area and, consequently, the mass and the heat transfer is greater. As a result, the condensation rate of bubbles in the subcooled region is higher. On the other hand, the void fraction in the superheated region near the heated wall is greater for simulations with smaller bubble size. From Figure 10 it can be seen that void fraction in the centre of the subchannel is higher in case of NEPTUNE_CFD simulations with large bubbles (i.e. 0.2mm and 0.3mm). It is due to the fact that larger bubbles are less condensable in liquid subcooled region than those generated by Yao-Morel and Ruyer-Seiler models. Similar conclusions were drawn by Peréz et al. [3].

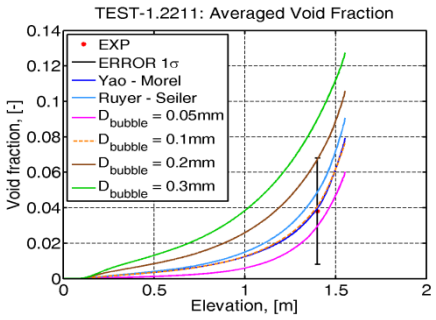

Figure 8: Axial evolution of cross-section averaged void fraction

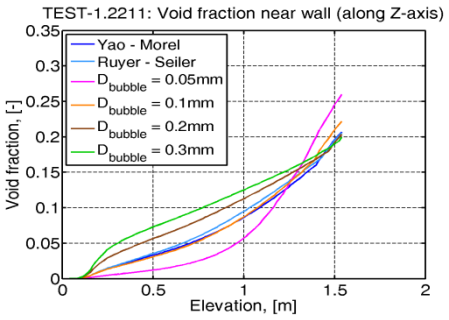

Figure 9: Axial evolution of void fraction at the near wall region

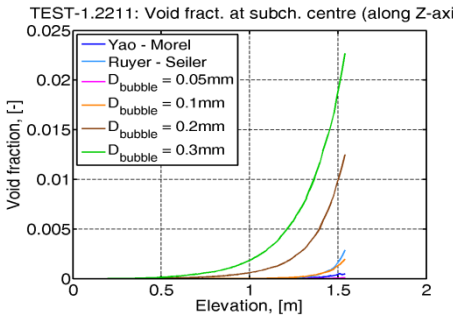

Figure 10: Axial evolution of void fraction at the centre of the subchannel

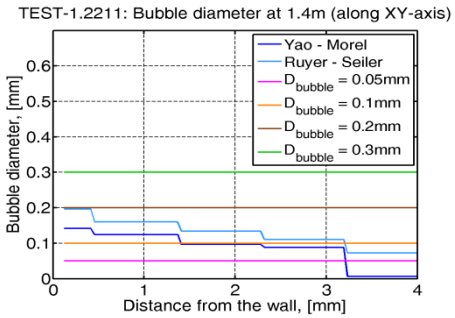

Figure 11: Bubble diameter size in the near wall region at 1.4m elevation

3.4 Effect of the Turbulence Model for Liquid Phase

The effect of the turbulence model for continuous liquid field has been investigated by performing simulations of PSBT test 1.2211 using first-order standard *k*-ε and second-order RANS turbulence models (Rij-ε SSG). As it is illustrated in Figure 12, the highest averaged void fraction at the location of measuring section (1.4m) is obtained in simulation with Rij-ε SSG turbulence model. Bubble diameter calculated by the *k*-ε turbulence model at this elevation is lower than that in case of Rij-ε SSG model (Figure 13), leading to higher condensation rate of bubbles in the subcooled region and, therefore, to lower void fraction.

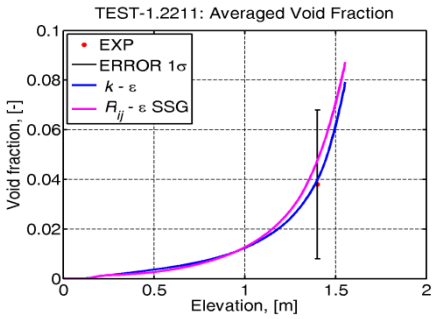

Figure 12: Axial evolution of cross-section averaged void fraction

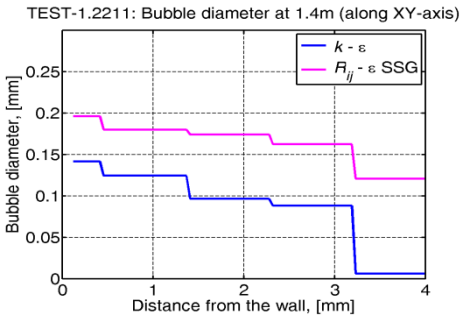

Figure 13: Bubble diameter size in the near wall region at 1.4m elevation

4 CALCULATION OF THE SELECTED PSBT TESTS

The results of the 42 selected PSBT tests are summarized in Figure 14 - Figure 15. As shown in Figure 14, the majority of code predictions are encompassed by the experimental uncertainty bands that represent the variation of the void fraction value by +/- 0.08 (i.e. +/- 8%, 2σ). Furthermore, the results of 25 tests are enveloped by the +/- 0.04 VF experimental uncertainty bands (i.e. +/-4%, 1σ).

Based on the results shown in Figure 15(a) it can be concluded that NEPTUNE_CFD code has a slight tendency toward underprediction of the void fraction with increase of the pressure (starting from ~ 122 bar). Besides, the code tends to underestimate the void fraction for the tests with a higher liquid mass flux (~3100 kg/m^2/s at the subchannel inlet, see Figure 15(b)). Regarding the influence of the flow subcooling on the calculation results, NEPTUNE_CFD code overpredicts the void fraction when increasing the inlet subcooling (Figure 15(c)). No explicit bias was found with the heat flux (Figure 15(d)).

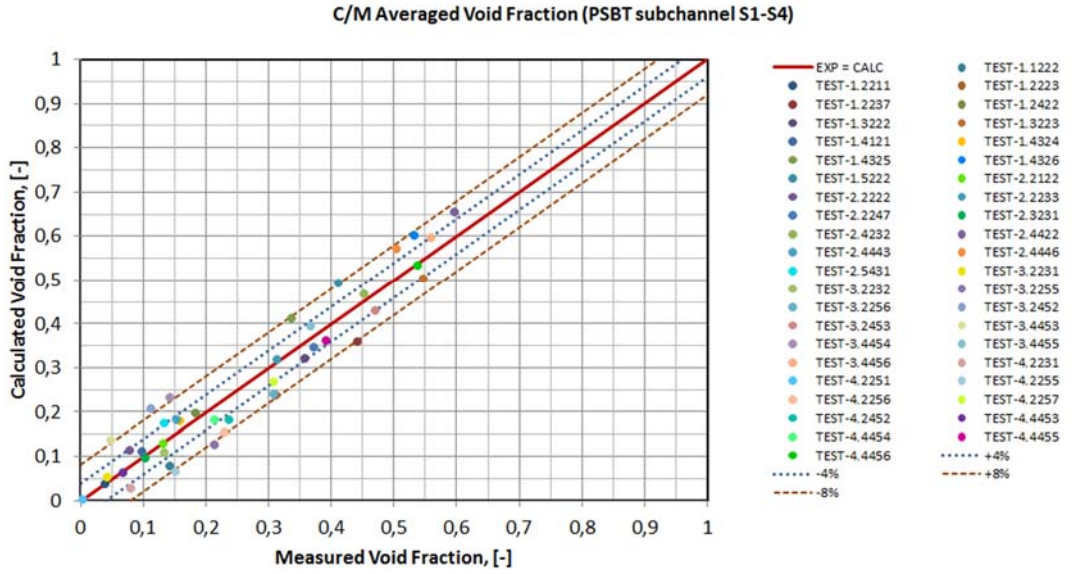

Figure 14: Axial evolution of cross-section averaged void fraction

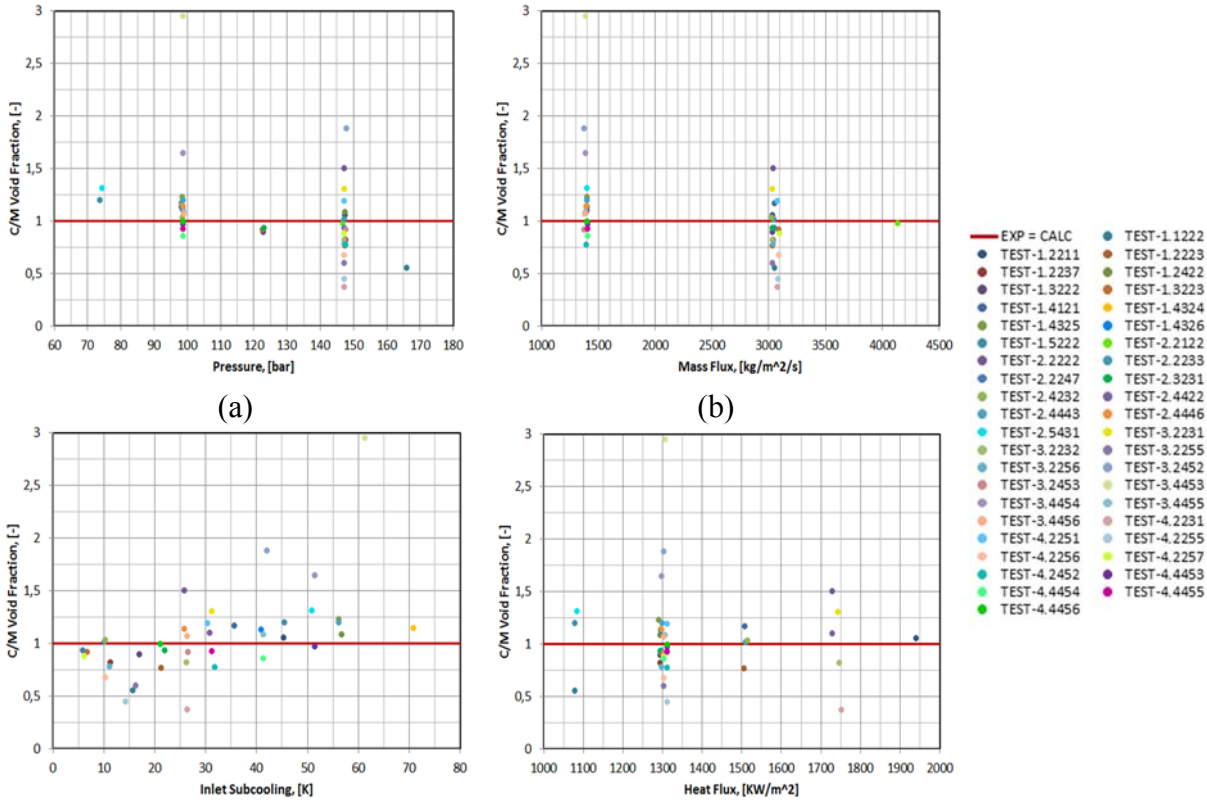

Figure 15: C/M Averaged Void Fraction at 1.4m elevation versus:
a) Pressure, b) Mass Flux, c) Inlet Subcooling, d) Heat Flux

5 CONCLUSIONS

The present paper reports the results of the validation activity of NEPTUNE_CFD v2.0.1 code against experimental data available from the OECD/NRC PSBT benchmark. From overall 126 experiments covering wide range of operating conditions, the 42 tests have been selected and simulated enveloping all 4 geometrical configurations of the subchannel. The majority of code predictions are encompassed by the experimental uncertainty bands that represent the variation of the void fraction (VF) value by +/- 0.08 (i.e. +/-8%, 2σ). The results of 25 tests are enveloped by the +/- 0.04 VF experimental uncertainty bands (i.e. +/-4%, 1σ). Generally, the code has a slight tendency to void fraction underprediction while increasing the pressure (starting from ~ 122 bar). The same trend was found for the tests at higher inlet mass flux (~3100 kg/m2/s). Besides, NEPTUNE_CFD code overpredicts the void fraction when increasing the inlet subcooling. No explicit bias was found with the heat flux.

Following the NEA/CSNI best practice guidelines about the computational grid design and grid quality, a mesh sensitivity analysis based on PSBT test 1.2211 has been performed. The axial mesh sensitivity study does not exhibit any significant change in the predicted results, however the void fraction calculated in the near-wall region is higher for grids with radial refinement. As a second step, series of sensitivity calculations of PSBT test 1.2211 have been performed in order to assess the effect of uncertainties of the experimental boundary and initial conditions on the code predictions. The biggest influence is observed in case of multi-parameter BC variations (by changing simultaneously subchannel pressure, inlet temperature, mass and heat fluxes). For instance, the calculated 0.04-wide variation for PSBT test 1.2211 represents approximately 50% of the nominal value ($VF_{nom} = 0.038$).

The influence of the implemented physical and closure models on NEPTUNE_CFD prediction has been studied. The largest impact on the calculated results is due to selected turbulence model for liquid phase and bubble size description model. The performed investigations have shown the ability of NEPTUNE_CFD code to predict reasonably the void fraction in PSBT subchannel using appropriate modelling.

ACKNOWLEDGMENTS

This work has been performed in the framework of the NURESAFE European collaborative project, financially supported by the European Commission.

REFERENCES

[1] A. Rubin, A. Schoedel, M. Avramova et al., “OECD/NRC Benchmark based on NUPEC PWR subchannel and bundle test (PSBT),” NEA-1849 ZZ-PSBT, 2010.

[2] C. Baudry et al., “Numerical Study of the Steady-State Subchannel Test-Case with NEPTUNE_CFD for the OECD/NRC NUPEC PSBT Benchmark”, Science and Technology of Nuclear Installations, Vol. 2012, doi:10.1155/2012/524598, 2012.

[3] J. Peréz et. al., “Validation of NEPTUNE-CFD Two-Phase Flow Models Using Experimental Data”, Science and Technology of Nuclear Installations, Vol. 2014, doi:10.1155/2014/185950, 2014.

[4] A. Guelfi et al., “NEPTUNE: a new software platform for advanced nuclear thermal hydraulics,” Nuclear Science and Engineering, Vol. 156, no. 3, pp. 281–324, 2007.

[5] EDF R&D, “NEPTUNE CFD version 2.0.1 theory guide”, EDF Fluid Dynamics, Power Generation and Environment Department, Multi-Phase Flow Group, June 24, 2013.

[6] EDF R&D, “NEPTUNE CFD version 2.0.1 user guide”, EDF Fluid Dynamics, Power Generation and Environment Department, Multi-Phase Flow Group, June 24, 2013.

[7] J. Mahaffy et al., Best Practice Guidelines for the Use of CFD in Nuclear Reactor Safety Applications, NEA/CSNI/R(2007)5, April 2007.

[8] M. Ishii and N. Zuber, “Drag coefficient and relative velocity in bubbly, droplet or particulate flows,” AIChE Journal, Vol. 25, no. 5, pp. 843–855, 1979.

[9] N. Zuber, “On the dispersed two-phase flow in the laminar flow regime,” Chemical Engineering Science, Vol. 19, no. 11, pp.897–917, 1964.

[10] A. Tomiyama et. al., “Transverse migration of single bubbles in simple shear flows,” Chemical Engineering Science, Vol. 57, no. 11, pp. 1849–1858, 2002.

[11] W. Yao and C. Morel, “Volumetric interfacial area prediction in upward bubbly two-phase flow”, Int. Journal of Heat and Mass Transfer, Vol. 47, no. 2, pp. 307–328, 2004.

[12] N. Kurul and M. Podowski, “Multidimensional effects in forced convection subcooled boiling,” Proc. 9th Int. Heat Transfer Conf., Jerusalem, Israel, 1990.

[13] Y. Egorov and F. Menter. “Experimental Implementation of the RPI wall boiling model CFX-5.6”, Technical Report ANSYS/TR-04-10, ANSYS GmbH, 2004.

[14] P. Ruyer, et al., “A bubble size distribution model for the simulation of bubbly flows”, Proc. 6th Int. Conf. on Multiphase Flows, Leipzig, Germany, 2007.